# Photochemical Removal of Formaldehyde in Air by Using a 172 nm Xe<sub>2</sub> Excimer Lamp

Masaharu TSUJI\*1,2† and Masato MIYANO\*3 †E-mail of corresponding author: tsuji@cm.kyushu-u.ac.jp

(Received May 20, 2025, accepted June 4, 2025)

The photochemical removal of formaldehyde (HCHO) was investigated in air (20 or 1%  $O_2$ ) using a side-on type of 172 nm vacuum ultraviolet (VUV)  $Xe_2$  excimer lamp at atmospheric pressure. Experiments were carried out in a closed batch system and a flow system. HCHO was finally oxidized to  $CO_2$  via HCHO, HCOOH, and CO intermediates at HCHO concentrations of 145 or 113 ppm. It was found that the initial  $O(^3P)$  + HCHO  $\rightarrow$  OH + CHO reaction and the subsequent OH + HCHO  $\rightarrow$  CHO + H<sub>2</sub>O reaction play major roles in the initial stage of the decomposition of HCHO. At 1%  $O_2$ , direct VUV photolysis of HCHO and HCOOH also participates in the removal pathways of HCHO. The removal rate constant of HCHO at 1%  $O_2$ , 25.0 min<sup>-1</sup>, was 3.5 times larger than 7.2 min<sup>-1</sup> at 20%  $O_2$ . When the HCHO removal was attempted using a flow system at a low HCHO concentration of 16 ppm, it was completely removed in the flow rate range of 1000–2000 ccm.

**Key words:** Indoor pollution, VOC, Formaldehyde, Oxidation, VUV photolysis, 172 nm Xe<sub>2</sub> excimer lamp, O(<sup>3</sup>P) atoms, OH radicals, CO, CO<sub>2</sub>, Batch system, Flow system

### 1. Introduction

Formaldehyde (HCHO) is a typical volatile organic compound (VOC). It is widely used for the production of organic chemicals, synthetic/artificial leather, textiles, pesticides, paints, adhesives, inks, and electronic equipment. In view of its widespread use, toxicity, and volatility, HCHO poses a significant danger to human health even at low levels. HCHO is also a causative agent of indoor pollution of air, because it liberates from tobacco smoke, furniture, and other consumer goods in houses.

Extensive studies have been conducted using effective and economically reasonable techniques for HCHO removal in air. Conventional HCHO removal techniques are absorption, physisorption, chemisorption, biological and botanical filtration, photocatalytic decomposition, membrane separation, plasma, and catalytic oxidation. 1-6)

We have recently used 172 nm VUV excimer lamps to remove such hydrocarbons and aldehydes as CH<sub>4</sub>, C<sub>2</sub>H<sub>4</sub>, C<sub>6</sub>H<sub>6</sub>, CH<sub>3</sub>CHO, and

 $C_2H_3CHO.^{7\cdot 12)}$  They could efficiently be decomposed and finally oxidized to  $CO_2$  in air at atmospheric pressure without using any expensive noble-metal catalysts. In the present study, we attempt to use a 172 nm  $Xe_2$  excimer lamp with a photon energy of 7.21 eV as a new photochemical removal method of HCHO in air at atmospheric pressure.

Previous UV + VUV photolysis of HCHO in air was carried out by using a mixture of 254 + 185 nm light from mercury lamps and photocatalysts.<sup>2-6)</sup> The threshold wavelengths for the formation of  $O(^3P)$  and  $O(^1D)$  from photolysis of  $O_2$  are as follows.<sup>13)</sup>

$$O_2 + hv \le 242.4 \text{ nm}: \ge 5.11 \text{ eV})$$
  
 $\rightarrow O(^3P) + O(^3P)$  (1)  
 $O_2 + hv \le 175.0 \text{ nm}: \ge 7.08 \text{ eV})$   
 $\rightarrow O(^3P) + O(^1D)$  (2)

On the basis of these facts,  $O_2$  cannot be decomposed into  $O(^3P) + O(^3P)$  at 254 nm (4.88 eV), whereas it can be decomposed into  $O(^3P) + O(^3P)$  at 185 nm (6.70 eV) with a small absorption cross section.<sup>13)</sup>

$$O_2$$
 + hv (185 nm)  $\rightarrow$  O(3P) + O(3P) (3)   
 $\sigma_3 \approx 3.3 \times 10^{-20} \text{ cm}^2 \text{ molecule}^{-1}$ 

Although previous investigators reported that O<sub>2</sub> is decomposed into O(<sup>3</sup>P) + O(<sup>1</sup>D) at 185

<sup>\*1</sup> Institute for Materials Chemistry and Engineering, and Research and Education Center of Green Technology

<sup>\*2</sup> Department of Applied Science for Electronics and Materials

<sup>\*3</sup> Department of Applied Science for Electronics and Materials, Graduate Student

nm,<sup>3-5)</sup> it is energetically impossible.

$$O_2 + hv (185 \text{ nm})$$
  
 $\Rightarrow O(^3P) + O(^1D) - 0.38 \text{ eV}$  (4)

Therefore, the contribution of O(1D) atoms in the HCHO removal by 185 nm photolysis was overestimated. Reaction mechanisms of HCHO under 185 nm photolysis in Refs. 3–5 should be revised.

O<sub>2</sub> is selectively decomposed into O(<sup>3</sup>P) + O(<sup>1</sup>D) at 172 nm with a larger absorption cross section.<sup>13,14)</sup>

$$O_2 + hv (172 \text{ nm}) \rightarrow O(^3P) + O(^1D)$$
 (5)  
 $\sigma_5 \approx 4.63 \times 10^{-19} \text{ cm}^2 \text{ molecule}^{-1}$ 

Since the absorption cross section of process (5) is 14 times larger than that of process (3), 172 nm light is expected to be more suitable than 185 nm one for the HCHO removal. In addition, mercury-free process is desirable as an ecofriendly photochemical removal technique.

The major purpose of this study is to obtain fundamental information on photochemical reactions of HCHO under irradiation of 172 nm Xe<sub>2</sub> excimer lamp in air. Not only direct VUV photochemical reactions of HCHO, but also reactions of O(<sup>3</sup>P,<sup>1</sup>D), OH, and O<sub>3</sub> with HCHO may contribute to the decomposition and oxidation of HCHO. Major photochemical reaction pathways of HCHO in air are discussed. All reaction rate constants and branching ratios of products used for discussion have been measured at about 300 K.<sup>15</sup>

# 2. Experimental

VUV photolysis apparatus used in this work was the same as that reported previously.<sup>8,9)</sup> Lights from an unfocused side-on type of 172 nm Xe<sub>2</sub> lamp (UER20H172; Ushio Inc) were used to remove HCHO at room temperature. Experiments were carried out in a closed batch system and a flow system. The chamber volume was changed by inserting different size of stainless-steel disks. Batch experiments were conducted at a chamber volume of 235.5 cm<sup>3</sup> and a chamber thickness of 3 cm, whereas flow experiments were carried out at a chamber volume of 39.3 cm3 and a chamber thickness of 0.5 cm.8 The total pressure was maintained at atmospheric pressure. The O2 concentration was 20 or 1% in the batch experiments, whereas it was 1% in the flow experiments. The HCHO concentrations were 145 or 113 ppm in the batch experiments and 16 ppm in the flow

experiment. The flow rate was varied from 1000 to 5000 ccm in the flow experiment.

Sample gases before and after photoirradiation were analyzed by a HORIBA gas analysis system (FG122-LS) equipped with an FTIR spectrometer. The IR spectra were measured in the 980-4000 cm<sup>-1</sup> region with an optical resolution of 4 cm<sup>-1</sup>. The concentrations of HCHO, HCOOH, CO, CO2, and O3 were determined from peak intensities of each FTIR band. The concentrations of HCHO, CO, and CO<sub>2</sub> were calibrated using their standard samples supplied from gas companies. The concentrations of HCOOH and O3 were evaluated by reference to the standard spectral data supplied by HORIBA Ltd.

The following gases were used without further purification: N<sub>2</sub> (purity >99.9998%; Taiyo Nippon Sanso (TNS) Corp.), O<sub>2</sub> (>99.99995%; TNS Corp.), HCHO (4840 ppm in high purity N<sub>2</sub>; TNS Corp.). HCHO was diluted in air (20 or 1% O<sub>2</sub>) before use.

### 3. Results and discussion

### 3.1 HCHO removal in the batch system

Figures 1(a)-1(d) show FTIR spectra of HCHO (145 ppm) in air (20% O<sub>2</sub>) before and after photoirradiation for 1, 10, and 30 s, respectively. Before photoirradiation, strong and weak HCHO bands are observed in the 1650-1830 and 2700-3000 cm<sup>-1</sup> regions, respectively. After photoirradiation for 1 s, the HCHO bands reduce their intensity by about 15%, whereas O<sub>3</sub> bands appear. With increasing the photoirradiation time from 1 s to 10 and 30 s, the HCHO bands decrease and disappear, O<sub>3</sub> bands become strong, and CO<sub>2</sub>, CO, and HCOOH bands appear.

Figures 2(a) and 2(b) show the dependence of concentrations of HCHO, CO, CO<sub>2</sub>, HCOOH, and  $O_3$  on the irradiation time in air (20%  $O_2$ ) in the 0-50 and 0-600 s ranges, respectively. In Fig. 2(a), the concentration of HCHO almost linearly decreases from 145 ppm to 10 ppm with increasing the irradiation time until 18 s, and then slowly decreases to zero at 30 s. The concentration of CO increases to 229 ppm until 18 s and slowly decreases to 218 ppm in the 20-50 s range. The concentration of CO<sub>2</sub> increases almost linearly to 112 ppm until 50 s. The concentration of HCOOH increases to 78 ppm at 16 s, and then decreases to zero in the 16–35 s range. The concentration of O₃ linearly increases to 2.2% after 50 s.

At longer irradiation times shown in Fig. 2(b), the concentration CO decreases from 218 ppm

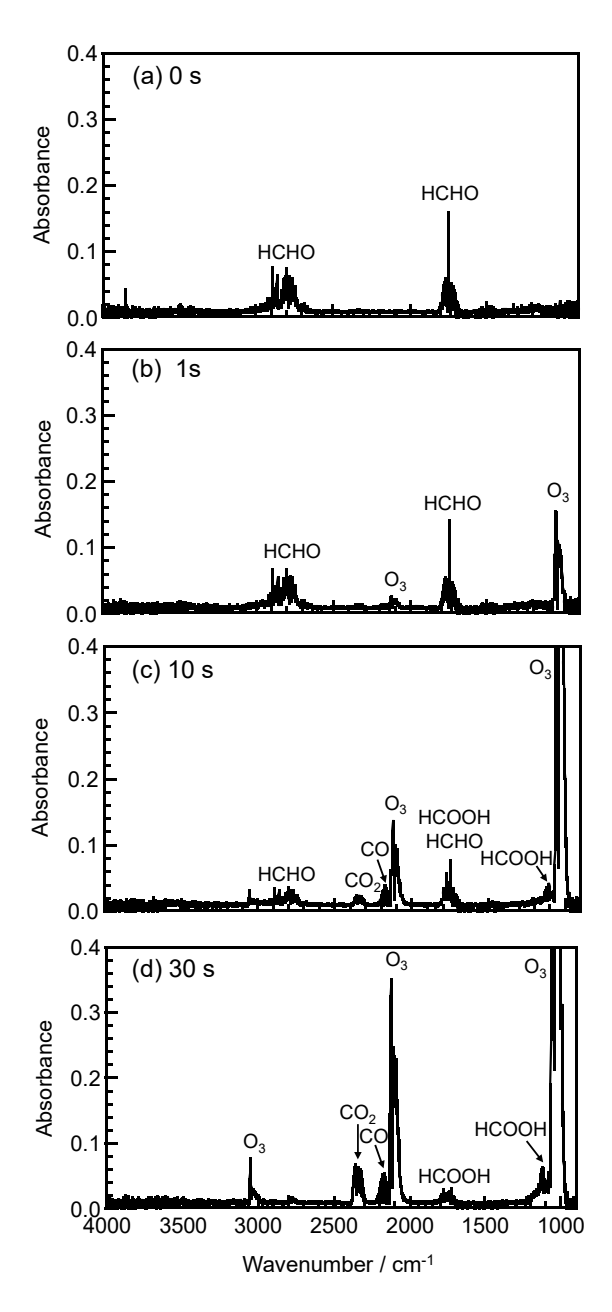
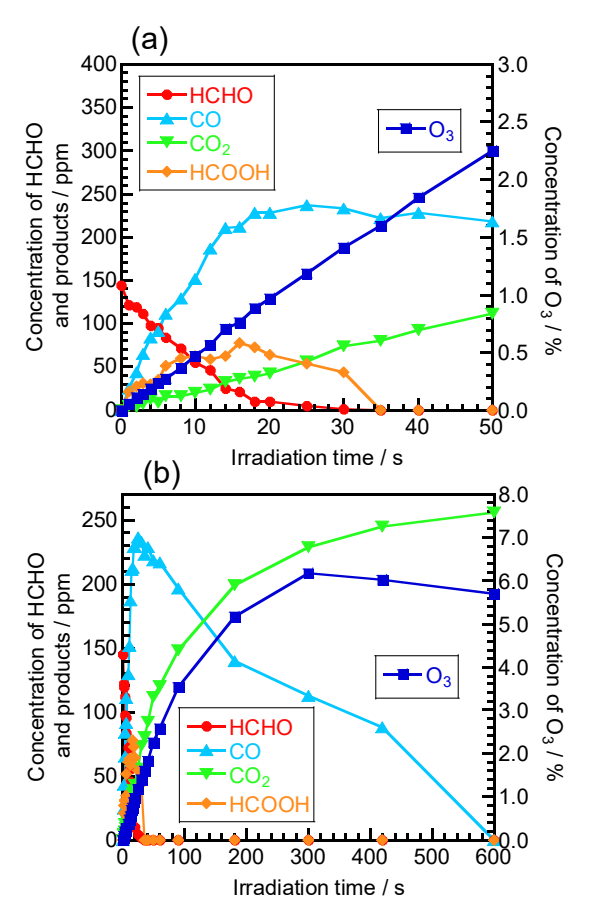


Fig. 1. (a) FTIR spectrum of HCHO in air (20% O<sub>2</sub>) (a) before photoirradiation and (b)-(e) after photoirradiation for 1, 10, and 30 s, respectively.

to zero in the 50--600 s range. The concentration of  $CO_2$  increases from 112 ppm to 255 ppm in the 50--600 s range. The concentration of  $O_3$  increases from 2.2 to 6.2% in the 50--300 s range, and then slowly decreases to 5.7% in the 300--600 s range. Time profiles of concentrations of HCHO, CO,  $CO_2$ , and HCOOH suggest that HCHO is finally oxidized to  $CO_2$  via HCOOH and CO intermediates.

The removal of HCHO in air was also studied



**Fig. 2**. Dependence of concentrations of HCHO, products, and  $O_3$  on the irradiation time in air (20%  $O_2$ ) in the (a) 0–50 s and (b) 0–600 s ranges.

at a low O<sub>2</sub> concentration of 1%, because the removal rates of CH<sub>3</sub>CHO and C<sub>2</sub>H<sub>3</sub>CHO at 1% O<sub>2</sub> were faster than those at 20% O<sub>2</sub>.<sup>9,10)</sup> Figures 3(a)-3(d) show FTIR spectra of HCHO (113 ppm) before and after photoirradiation for 1, 2, and 5 s, respectively. Before photoirradiation, HCHO bands are observed in the 1650-1830 and 2700-3000 cm<sup>-1</sup> regions. A residual impurity band of H<sub>2</sub>O is partially overlapped with the main HCHO band in the 1650-1830 cm<sup>-1</sup> range. It should be noted that the removal rate of HCHO at 1% O<sub>2</sub> is faster than that at 20% O<sub>2</sub>. After photoirradiation for 1 s, the HCHO bands decrease in their intensities by about 50%, whereas CO<sub>2</sub> CO, and O<sub>3</sub> bands appear. It should be noted that HCOOH band, which is observed at 20% O<sub>2</sub>, is not detected at 1% O<sub>2</sub>. With increasing the photoirradiation time from 1 to 2 s, HCHO bands decrease, whereas CO<sub>2</sub>, CO, and O<sub>3</sub> bands become strong. Further increasing the irradiation time from 2 to 5 s, HCHO bands disappear, whereas CO<sub>2</sub>, CO, and O<sub>3</sub> bands further increase.

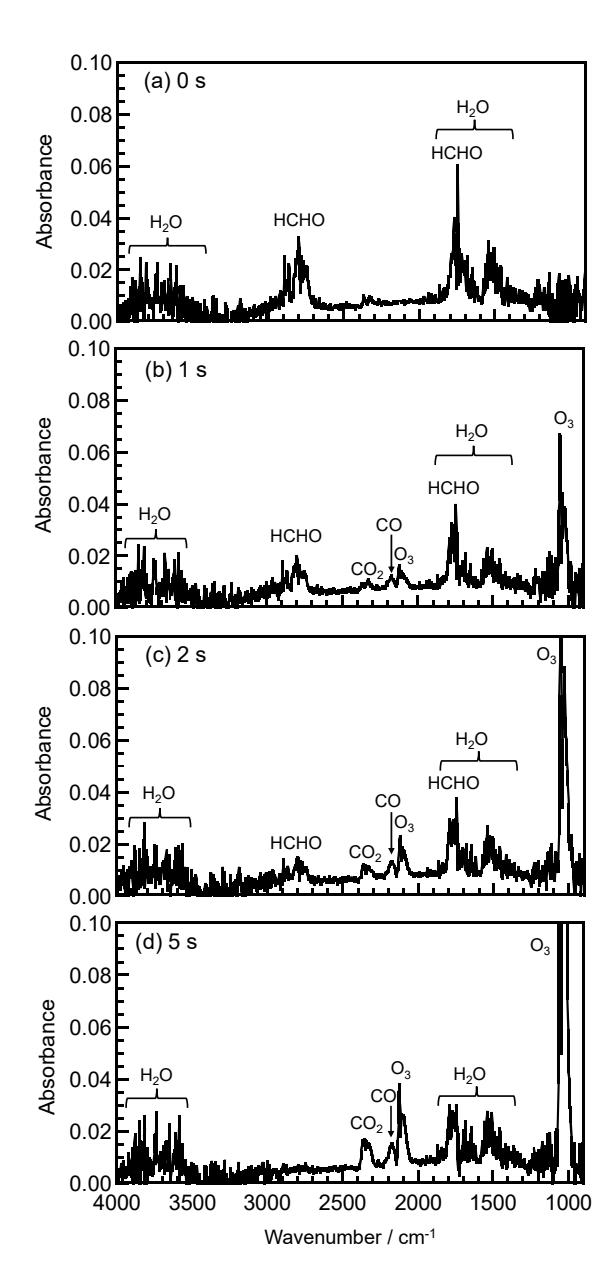


**Fig. 3.** (a) FTIR spectrum of HCHO in O<sub>2</sub> (1%) (a) before photoirradiation and (b)–(d) after photoirradiation for 1, 2, and 5 s, respectively.

Figure 4 shows the dependence of concentrations of HCHO, CO, CO<sub>2</sub>, and O<sub>3</sub> on the irradiation time. The concentration of HCHO rapidly decreases from 113 ppm to zero at 5 s. The concentration of CO increases to 174 ppm until 7 s and slowly decreases to 150 ppm in the 7–10 s range. The concentration of CO<sub>2</sub> increases linearly to 30 ppm until 10 s. These time profiles suggest that HCHO is oxidized to CO<sub>2</sub> via CO. An outstanding feature of HCHO removal at 1% O<sub>2</sub> is that [CO]/[CO<sub>2</sub>] ratios at 1–5 s are larger than those at 20% O<sub>2</sub> by factors of 1.5–4.7. This suggests that an additional

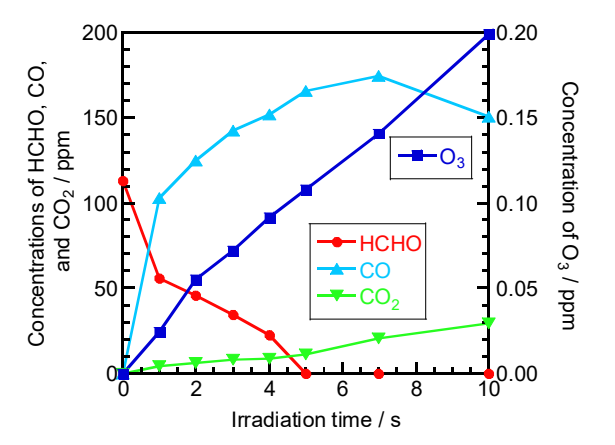


Fig. 4. Dependence of concentrations of HCHO, products, and  $O_3$  on the irradiation time in air (1%)  $O_2$  in the 0-10 s range.

process takes part in the formation of CO at 1% O<sub>2</sub>. The concentration of O<sub>3</sub> linearly increases to 0.2% after 10 s.

Assuming a pseudo-first order reaction,  $^{9,10)}$  initial removal rate constants of HCHO were determined to be 7.2 min<sup>-1</sup> at 20%  $O_2$  in the 0–18 s range and 25.0 min<sup>-1</sup> at 1%  $O_2$  in the 0–4 s range. This indicates that the removal rate constant of HCHO at 1%  $O_2$  is larger than that at 20%  $O_2$  by a factor of 3.5.

# 3.2 Possible removal mechanisms of HCHO under 172 nm photolysis in air

Under 172 nm photolysis of HCHO (145 or 113 ppm) in  $N_2/O_2$  mixtures (20 or 1%  $O_2$ ), the 172 nm light is initially absorbed by HCHO and  $O_2$ , because  $N_2$  has no absorption for the 172 nm light. In general, the total photon energy absorbed by such a mixture as HCHO and  $O_2$  during passing through the decomposition chamber,  $E_{total}$ , is calculated from the relation:

$$E_{total} = E_0 - E_0 \exp(-l\sum_i \sigma_i N_i)$$
 (6)

Here,  $E_0$ , l,  $\sigma_i$ , and  $N_i$ , are the energy of excimer lamp, the length of decomposition chamber, absorption cross section of a molecule i, and its number density, respectively. Photon energy absorbed by a molecule i,  $E_i$ , is obtained from the relation.

$$E_i = E_{total} \times \frac{\sigma_i N_i}{\sum_i \sigma_i N_i} \tag{7}$$

 $\sigma_{\rm HCHO}$  and  $\sigma_{\rm O_2}$  values at 172 nm were reported to be  $8.1\times10^{-18}$  and  $4.63\times10^{-19}$  cm² molecule<sup>-1</sup>, respectively.<sup>13,16)</sup> When we calculated  $E_{\rm HCHO}$  /  $(E_{\rm HCHO}+E_{\rm O_2})$  and  $E_{\rm O_2}$  /  $(E_{\rm HCHO}+E_{\rm O_2})$  values at 172 nm using these

values at HCHO concentrations of 145 and 113 ppm, they are 1 and 99% at 20%  $O_2$ , and 17 and 83% at 1%  $O_2$ , respectively. These values imply that most photons are absorbed by  $O_2$  at 20%  $O_2$ , whereas 17% of incident photons is absorbed by HCHO at 1%  $O_2$  in the initial stage.

Photolysis of HCHO at 20%  $O_2$  starts from selective photolysis of  $O_2$  into  $O(^3P) + O(^1D)$  under 172 nm photoirradiation: process (5). Metastable  $O(^1D)$  atoms are rapidly quenched to the ground  $O(^3P)$  atoms by collisions with  $N_2$  and  $O_2$  atoms in air.

$$O(^{1}D) + N_{2} \rightarrow O(^{3}P) + N_{2}$$
 (8)  
 $(k_{8} = 2.59 \times 10^{-11} \text{ cm}^{3} \text{ molecule}^{-1} \text{ s}^{-1})^{15)}$ 

$$O(^{1}D) + O_{2} \rightarrow O(^{3}P) + O_{2}$$
 (9)  
 $(k_{9} = 4.05 \times 10^{-11} \text{ cm}^{3} \text{ molecule}^{-1} \text{ s}^{-1})^{15)}$ 

The rate constants and products of the  $O(^{3}P)/HCHO$  reaction have been measured.

O(3P) + HCHO 
$$\rightarrow$$
 HCO + OH  
 $(k_{10} = 1.67 \times 10^{-13} \text{ cm}^3 \text{ molecule}^{-1} \text{ s}^{-1})^{15)}$  (10)

OH radicals formed in reaction (10) further react with HCHO.

OH + HCHO 
$$\rightarrow$$
 HCO + H<sub>2</sub>O (11)  
( $k_{11} = 9.38 \times 10^{-12} \text{ cm}^3 \text{ molecule}^{-1} \text{ s}^{-1}$ )<sup>15)</sup>

Since the OH/HCHO reaction (11) is faster than the O(<sup>3</sup>P)/HCHO reaction (10) by a factor of 56, it is expected that not only the O(<sup>3</sup>P)/HCHO reaction (10) but also the OH/HCHO reaction (11) play major roles in the initial oxidation processes of HCHO. The same HCO radical is formed in reactions (10) and (11). It is further oxidized to CO by the fast HCO/O<sub>2</sub> reaction.

HCO + O<sub>2</sub> 
$$\rightarrow$$
 CO + HO<sub>2</sub> (12)  
( $k_{12} = 5.20 \times 10^{-12} \text{ cm}^3 \text{ molecule}^{-1} \text{ s}^{-1}$ )<sup>15)</sup>

CO is finally converted to CO<sub>2</sub> by the two-body and three-body reactions.

O(<sup>1</sup>D) + CO 
$$\rightarrow$$
 CO<sub>2</sub> (13)  
( $k_{13} = 8.00 \times 10^{-11} \text{ cm}^3 \text{ molecule}^{-1} \text{ s}^{-1})^{15}$ )

OH + CO 
$$\rightarrow$$
 CO<sub>2</sub> + H (14)  
( $k_{14} = 1.48 \times 10^{-13} \text{ cm}^3 \text{ molecule}^{-1} \text{ s}^{-1})^{15}$ )

CO + O + N<sub>2</sub> 
$$\rightarrow$$
 CO<sub>2</sub> + N<sub>2</sub> (15a)  
( $k_{15a} = 6.89 \times 10^{-36} \text{ cm}^6 \text{ molecule}^{-2} \text{ s}^{-1}$ )<sup>15)</sup>

CO + O + O<sub>2</sub> 
$$\rightarrow$$
 CO<sub>2</sub> + O<sub>2</sub> (15b)  
( $k_{15b} = 2.81 \times 10^{-35} \text{ cm}^6 \text{ molecule}^{-2} \text{ s}^{-1}$ )<sup>15)</sup>

Here, the  $k_{15b}$  value at 300 K was estimated by extrapolating the equation reported in the 373–525 K range.<sup>15,17)</sup> On the basis of above reactions, the formation of CO<sub>2</sub> from HCHO proceeds via HCHO  $\rightarrow$  CHO  $\rightarrow$  CO  $\rightarrow$  CO<sub>2</sub> oxidation processes, where HCOOH is not involved as an intermediate.

The OH/HCO reaction is the most possible formation process of HCOOH under 172 nm photolysis of a HCHO/O<sub>2</sub> mixture.

OH + HCO 
$$\rightarrow$$
 HCOOH (16)  
( $k_{16} = 9.20 \times 10^{-13} \text{ cm}^3 \text{ molecule}^{-1} \text{ s}^{-1})^{15}$ 

HCOOH molecules are oxidized by the following processes.

OH + HCOOH 
$$\rightarrow$$
 HCOO + H<sub>2</sub>O (17)  
( $k_{17} = 5.66 \times 10^{-13} \text{ cm}^3 \text{ molecule}^{-1} \text{ s}^{-1})^{15}$ )

$$O(^{3}P) + HCOO \rightarrow CO_{2} + OH$$
 (18)  
 $(k_{18} = 1.44 \times 10^{-11} \text{ cm}^{3} \text{ molecule}^{-1} \text{ s}^{-1})^{15})$ 

As shown above reactions, the formation of  $CO_2$  proceeds through  $HCOOH \rightarrow HCOO \rightarrow CO_2$ , where CO is not involved as an intermediate.

At 1% O<sub>2</sub>, besides above reactions, direct photolysis of HCHO by the 172 nm light contributes to the removal of HCHO. Possible photolysis processes of HCHO as follows.

$$HCHO + hv(172 \text{ nm}) \rightarrow HCO + H$$
 (19a)  
  $\rightarrow CO + H_2$  (19b)

Based on reported VUV photolysis study by Sperling and Toby,  $^{18)}$  process (19a) is dominant at 254 nm, whereas process (19b) is main at 147 nm. Under 172 nm photolysis at 1%  $O_2$ ,  $[CO]/[CO_2]$  ratios below 5 s are larger than those at 20%  $O_2$ . It is therefore reasonable to assume that process (19b) contributes to the formation of CO at 1%  $O_2$ .

At 1%  $O_2$ , HCOOH is not detected. One reason for the absence of HCOOH is direct 172 nm photolysis of HCOOH with an absorption cross section of  $2.5 \times 10^{-18}$  cm<sup>2</sup> molecule<sup>-1</sup>.<sup>19)</sup> Schwel et al.<sup>20)</sup> reported that both HCOO + H and HCO + OH are major product channels of VUV photolysis of HCOOH in the 6–13 eV (95.3–207 nm) region.

HCOOH + hv(95.3-207 nm)  

$$\rightarrow$$
 HCOO + H (20a)  
 $\rightarrow$  HCO + OH (20b)

Therefore, it is expected that processes (20a) and (20b) occur at 172 nm (7.21 eV) photolysis of HCOOH at  $1\% O_2$ .

It is known that the  $O_3/HCHO$  reaction is very slow.

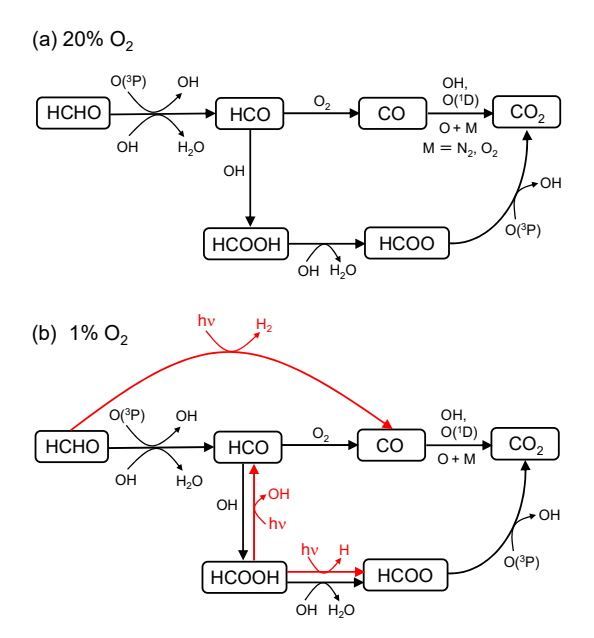
$$O_3 + HCHO \rightarrow Products$$
 (21)  
 $(k_{21} = 2.09 \times 10^{-24} \text{ cm}^3 \text{ molecule}^{-1} \text{ s}^{-1})^{15}$ 

When the O<sub>3</sub>/HCHO reaction is studied using the same technique as that reported previously,<sup>9)</sup> no reaction can be observed. This observation is consistent with its reported very small rate coefficient.

Schemes 1(a) and 1(b) summarize the major reaction processes of HCHO removal in air under 172 nm photolysis at 20 and 1% O<sub>2</sub>, respectively. Processes described by red lines in Scheme 1(b) are additional photolysis channels, which occur only at 1% O2. Although we do not show photolysis of O<sub>2</sub> and O<sub>3</sub> under 172 nm irradiation in Scheme 1, photolysis of a HCHO/O<sub>2</sub> mixture initiates from photodissociation of  $O_2$  into  $O(^3P) + O(^1D)$ , as we have recently reported in oxidation schemes of CH<sub>4</sub> and C<sub>2</sub>H<sub>4</sub> under 172 nm photolysis in air.11,12) At 20% O2, HCHO molecules are oxidized via two processes: HCHO  $\rightarrow$  HCO  $\rightarrow$  CO  $\rightarrow$  CO<sub>2</sub> and HCHO  $\rightarrow$  HCO  $\rightarrow$  HCOOH  $\rightarrow$  HCOO  $\rightarrow$  CO<sub>2</sub>, where major active species are O(³P), OH, and O<sub>2</sub>. OH radicals are mainly generated by the fast O(³P)/HCHO reaction (10). At 1% O<sub>2</sub>, besides processes observed at 20% O<sub>2</sub>, direct VUV photolysis of HCHO and HCOOH contributes to the removal of HCHO. The rapid formation of CO and absence of HCOOH at 1% can be explained by effects of direct photolysis of HCHO and HCOOH by 172 nm photons.

In Table 1 are compared the initial removal rate constants of HCHO at 20 and 1% O<sub>2</sub> with those of CH<sub>3</sub>CHO and C<sub>2</sub>H<sub>3</sub>CHO measured by using the same apparatus. At 20% O<sub>2</sub>, the removal rate constant of HCHO is larger than that of CH<sub>3</sub>CHO by a factor of 2.2, whereas it is smaller than that of C<sub>2</sub>H<sub>3</sub>CHO by 14%. At 1% O<sub>2</sub>, the removal rate constant of HCHO is larger than those of CH<sub>3</sub>CHO and C<sub>2</sub>H<sub>3</sub>CHO by 36 and 30%, respectively. These results suggest that HCHO can be oxidized efficiently as in the cases of CH<sub>3</sub>CHO and C<sub>2</sub>H<sub>3</sub>CHO both at 20 and 1% O<sub>2</sub>.

For all aldehydes we studied, removal rate constants at 1%  $O_2$  were larger than those at 20%  $O_2$ . There are two possible reasons for these results. One is a longer penetration length of incident light at 1%  $O_2$ .<sup>9)</sup> Therefore, the photolysis of HCHO can occur uniformly in a larger reaction volume at 1%  $O_2$ . The other



**Scheme 1.** Major oxidation processes of HCHO under 172 nm photolysis at (a) 20%  $O_2$  and (b) 1%  $O_2$  in air. Direct VUV photolysis processes, which take part in the HCHO removal only at 1%  $O_2$ , are described in red in (b).

reason is competition between (10) and (15a) + (15b).

$$O(^{3}P) + HCHO \rightarrow HCO + OH$$
 (10)

$$O(^{3}P) + O_{2} + O_{2} \rightarrow O_{3} + O_{2}$$
 (15a)

$$O(^{3}P) + O_{2} + N_{2} \rightarrow O_{3} + N_{2}$$
 (15b)

At 1%  $O_2$ , the relative contribution of reaction (10) to that of (15a) + (15b) is larger than that at 20%  $O_2$ , because three-body reactions (15a) + (15b) are greatly suppressed at 1%  $O_2$ . This is consistent with much lower concentration of  $O_3$  at 1%  $O_2$  than that at 20%  $O_2$ . This is the other reason for the larger removal rate constant of HCHO at 1%.

**Table 1**. Removal rate constants of aldehydes by using a side-on type of 172 nm excimer lamp at 20% or 1%  $O_2$ .

Aldehyde	$O_2$	Removal	
	fraction	rate constant	Ref.
	/ %	/ min <sup>-1</sup>	
НСНО	20	7.2	This
	1	25.0	work
CH <sub>3</sub> CHO	20	3.3	Ref.
	1	18.4	9
C <sub>2</sub> H <sub>3</sub> CHO	20	8.4	Ref.
	1	19.3	10

### 3.3 HCHO removal in the flow system

For actual application of the photochemical removal of formaldehyde, a flow system, by which continuous removal of HCHO gas is possible, is required. Figure 5(a) shows the dependence of the concentrations of HCHO, CO, CO<sub>2</sub>, and O<sub>3</sub> on the flow rate at an initial HCHO concentration of 16 ppm. Figure 5(b) shows the dependence of residual amount of HCHO, [HCHO]/[HCHO]<sub>0</sub>, on the flow rate. Here [HCHO]<sub>0</sub> denotes the initial concentration of HCHO. Results show that all HCHO is removed in the low flow rate range of 1000-2000 ccm. The concentration of HCHO increases from 6.6 ppm to 8.3 ppm with increasing the flow rate from 3000 to 5000 ccm, whereas those of CO, CO<sub>2</sub>, and O<sub>3</sub> decrease with increasing the flow rate from 1000 to 5000 ccm. Although all HCHO is removed in the low flow rate range of 1000-2000 ccm, the residual amount of HCHO increases from 36% to 42% in the 3000-5000 ccm range.

In the flow system, the irradiation time corresponds to the residence time of HCHO gas in the photolysis chamber. The average

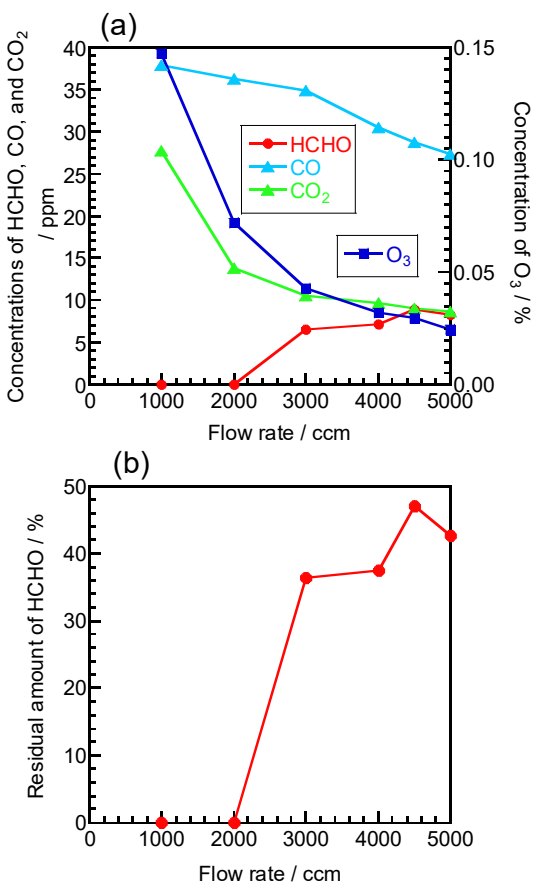


**Fig. 5**. (a) dependence of concentrations of HCHO, CO, and CO<sub>2</sub> on the flow rate. (b) dependence of residual amount of HCHO on the flow rate.

residence time of HCHO in the photolysis chamber, t, is estimated from the relation, t = V/v, where V is the total volume of the photolysis chamber and v is the flow rate. The residence time of HCHO in the photolysis chamber decreases concomitantly with increasing flow rate. Actually, at flow rates of 5000, 2000, and 1000 ccm, the t values were estimated respectively as 0.47, 1.2, and 2.4 s. Based on the results presented above, the HCHO removal in air is possible in the flow system at a low  $O_2$  concentration of 1% during short photoirradiation times of 1.2–2.4 s.

## 4. Summary and Conclusion

The photolysis of formaldehyde by using a side-on type of 172 nm  $Xe_2$  excimer lamp was studied in air (20 or 1%  $O_2$ ) at atmospheric pressure. We found that HCHO was oxidized to  $CO_2$  via HCO, HCOOH, and CO in air. In the presence of  $O_2$ ,  $O(^3P,^1D)$ , OH, and  $O_3$  can be active species for the removal of HCHO.

Results showed that  $O(^{3}P)$  and OH are major active species under the 172 nm photolysis of HCHO in the initial stage. At 1%  $O_{2}$ , direct 172 nm photolysis of HCHO also contributes to the HCHO dissociation.

The removal rate constant of HCHO at  $1\% O_2$  was 3.5 times faster than that at  $20\% O_2$  because of larger irradiation volume in the reaction chamber and slower loss of  $O(^3P)$  by the three-body  $O(^3P) + O_2 + M \rightarrow O_3 + M$  (M =  $N_2$  and  $O_2$ ) reactions. The removal rate constant of HCHO at  $20\% O_2$  was 2.2 times larger than that of  $CH_3CHO$ , whereas it was 14% smaller than that of  $C_2H_3CHO$ . The removal rate constant of HCHO at 1% was larger than those of  $CH_3CHO$  and  $C_2H_3CHO$  by 30-36%.

Photochemical removal of HCHO was also studied using a flow system at a low HCHO concentration of 16 ppm. It was completely removed in the flow rate range of 1000–2000 ccm. The present results demonstrate that mercury-free 172 nm Xe<sub>2</sub> excimer lamp is useful for the HCHO removal in air without using any expensive novel-metal catalysts.

### Acknowledgments

This work was supported by NEDO (project number NCJJ200049, 2008–2009) and City Area Project from Fukuoka Prefecture (2009).

#### References

- B. Robert and G. Nallathambi, *Environ. Chem. Lett.*, 19, 2551 (2021).
- 2) Q. Hong, S. Dezhi, and C. Guoqing, J. Environ. Sci., 19,

- 1136 (2007).
- 3) L. Yang, Z. Liu, J. Shi, Y. Zhang, H. Hu, and W. Shangguan, Sep. Purif. Techonol., 54, 204 (2007).
- P. Fu, P. Zhanga, and J. Li, Appl. Catal. B Environ., 105, 220 (2011).
- M. Y. Wang, Y. W. Lu, F. Wu, X. J Zhang, and C. X. Yang, Procedia Eng., 121, 521 (2015).
- S. Cheng, Y. Li, C. Yuan, P. Tsai, H. Shen, and C. Hung, Aerosol and Air Quality Research, 18, 3220 (2018).
- M. Tsuji, T. Kawahara, N. Kamo, and M. Miyano, *Bull. Chem. Soc. Jpn.*, 83, 582 (2010).
- 8) M. Tsuji, T. Kawahara, K. Uto, N. Kamo, M. Miyano, J. Hayashi, and T. Tsuji, *Environ. Sci. Pollut. Res.*, 25, 18980 (2018).
- M. Tsuji, M. Miyano, N. Kamo, T. Kawahara, K. Uto, J. Hayashi, and T. Tsuji, *Environ. Sci. Pollut. Res.*, 26, 11314 (2019).
- 10) M. Tsuji, M. Miyano, N. Kamo, T. Kawahara, K. Uto, J. Hayashi, and T. Tsuji, *Int. J. Environ. Sci. Technol.*, 16, 7229 (2019).
- M. Tsuji, N. Kamo, M. Miyano, and M. Kawahara, *Engineering Sciences Reports, Kyushu University*, 46, 19 (2024).
- 12) M. Tsuji, N. Kamo, and M. Miyano, *Engineering Sciences Reports, Kyushu University*, 47, 1 (2025).
- H. Okabe, "Photochemisty of Small Molecules", John Wiley & Sons, New York (1978).
- 14) J. B. Nee and P. C. Lee, J. Phys. Chem. A, 101, 6653 (1997).
- 15) NIST Chemical Kinetics Database on the Web, Standard Reference Database 17, Version 7.1 (Web Version), Release 1.6.8, Data Version 2024. http://kinetics.nist.gov/kinetics/index.jsp.
- 16) M. Suto, X. Wang, and L. C. Lee, J. Chem. Phys. 85, 4228 (1986).
- 17) V. N. Kondratev and I. L. Ptichkin, *Kinet. Katal.*, 2, 492 (1961).
- H. P. Sperling and S. Toby, Can. J. Chem., 51, 471 (1973).
- 19) M. Suto, X. Wang, and L. C. Lee, J. Phys. Chem., 92, 3764 (1988).
- 20) M. Schwell, F. Dulieu, H.-W. Jochims, J.-H. Fillion, J.-L. Lemaire, H. Baumgärtel, and S. Leach, J. Phys. Chem. A, 106, 10908 (2002).